

Electronic Supplementary Information

Cellular uptake of ribonuclease A-functionalised core-shell silica microspheres

Gwen F. Chimonides,^a Jonathan M. Behrendt,^b Evita Chundoo,^a Charlotte Bland,^c Anna V. Hine,^d Andrew Devitt,^c David A. Nagel,^d and Andrew J. Sutherland^{a*}

* Correspondence to: Andrew Sutherland, Chemical Engineering & Applied Chemistry, School of Engineering & Applied Science, Aston University, Birmingham, B4 7ET, UK.
E-mail: a.j.sutherland@aston.ac.uk

a Chemical Engineering & Applied Chemistry, School of Engineering & Applied Science, Aston University, Birmingham, B4 7ET, UK

b School of Chemistry, University of Manchester, Oxford Road, Manchester, M13 9PL, UK

c Aston Research Centre for Healthy Ageing & School of Life & Health Sciences, Aston University, Birmingham, B4 7ET, UK

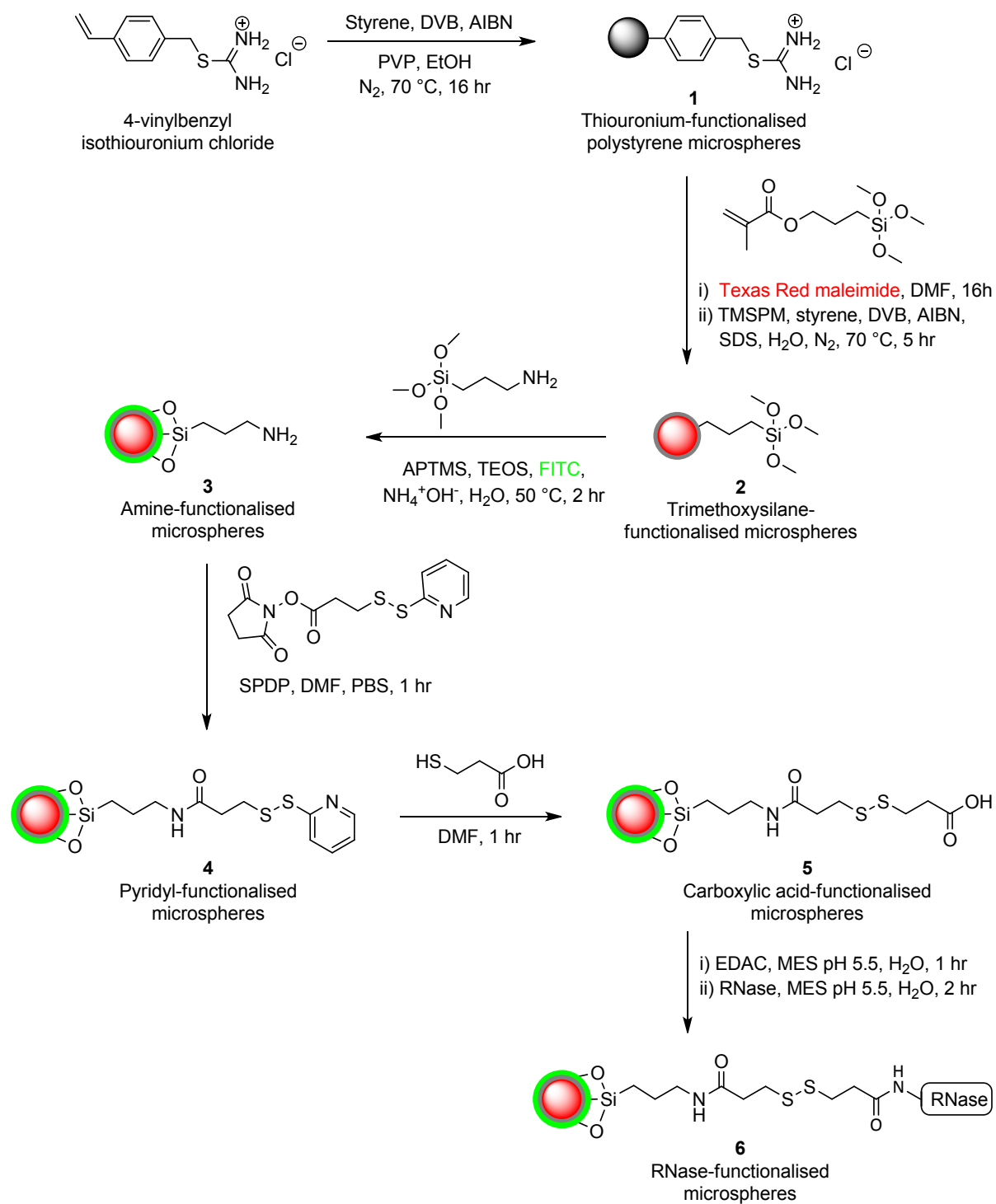
d School of Life & Health Sciences, Aston University, Birmingham, B4 7ET, UK

A visual guide to the fluorescently-labelled microspheres used in this study, a scheme of the full synthesis of RNase-functionalised microspheres **6**, characterisation of surface functionality, FTIR spectroscopy data, laser diffractometry data, TEM and energy dispersive x-ray analysis data, fluorescent labelling of RNase and micrographs that confirm internalisation of microspheres into cells are provided herein.

Table S1. A guide to the fluorescently-labelled microspheres used in this study.

Microspheres	[i]	a ^[ii]	b ^[iii]	c ^[iv]
1				
2				
3				
4				
5				
6				

[i] Microspheres **1** to **6** inclusive were synthesised to exemplify the multifunctional potential of our particles (Scheme 1 and Figure 1 in main manuscript); [ii] Microspheres **3a** to **6a** inclusive were synthesised to confirm the conjugation of RNase protein to the surface of our particles (Scheme 2 and Figure 2 in main manuscript); [iii] Microspheres **2b** to **6b** inclusive were synthesised without fluorophores for use in gel-electrophoresis (Figures 3 and 4 in main manuscript), cellular delivery for Acridine Orange staining assays (Figure 5 in main manuscript) amine-loading assays (Table S2 and Figure S2) and FTIR spectroscopy (Figure S3); [iv] Microspheres **3c** to **6c** inclusive were synthesised to confirm the internalisation of RNase-functionalised microspheres into HeLa cells (Figure S10) and for characterisation of carboxylic acid-functionalisation (Figure S1).



Scheme S1. Full synthesis of RNase-functionalised microspheres **6**.

EDAC coupling of BODIPY to carboxylic acid-functionalised microspheres 5c

The carboxylic acid-functionalised microspheres **5c** were conjugated to an amine-functionalised fluorophore in order to verify the presence of carboxylic acid moieties, and, in turn, the success of the modification steps. Trimethoxysilane-functionalised **2c**, amine-functionalised **3c**, pyridyl-functionalised **4c** and carboxylic acid-functionalised **5c** microspheres were all subjected to EDAC coupling to BODIPY, to highlight the difference in surface chemistry of the microsphere. Specifically, EDAC in distilled water (1 mg, 1 ml) was added to microspheres (**2c**, **3c**, **4c** and **5c**, separately) in MES solution (10 %, pH 5.5) (10 mg, 2 ml) and mixed with shaking for 5 hours at room temperature. The microspheres were washed twice with MES (10 %, pH 5.5) and resuspended in MES (10 %, pH 5.5). BODIPY in water 1 mg ml⁻¹ (20 µl) was added to the microsphere suspension and incubated at room temperature with shaking overnight. The microspheres were washed twice with distilled water (2 x 2 ml) and DMF (5 x 2 ml) and final resuspension in DMF (1 ml). BODIPY has a characteristic emission at 616 nm. As expected, inspection by fluorescence confocal microscopy shows successful conjugation with only the carboxylic acid-functionalised microspheres **5c**. Results are shown in Figure S1.

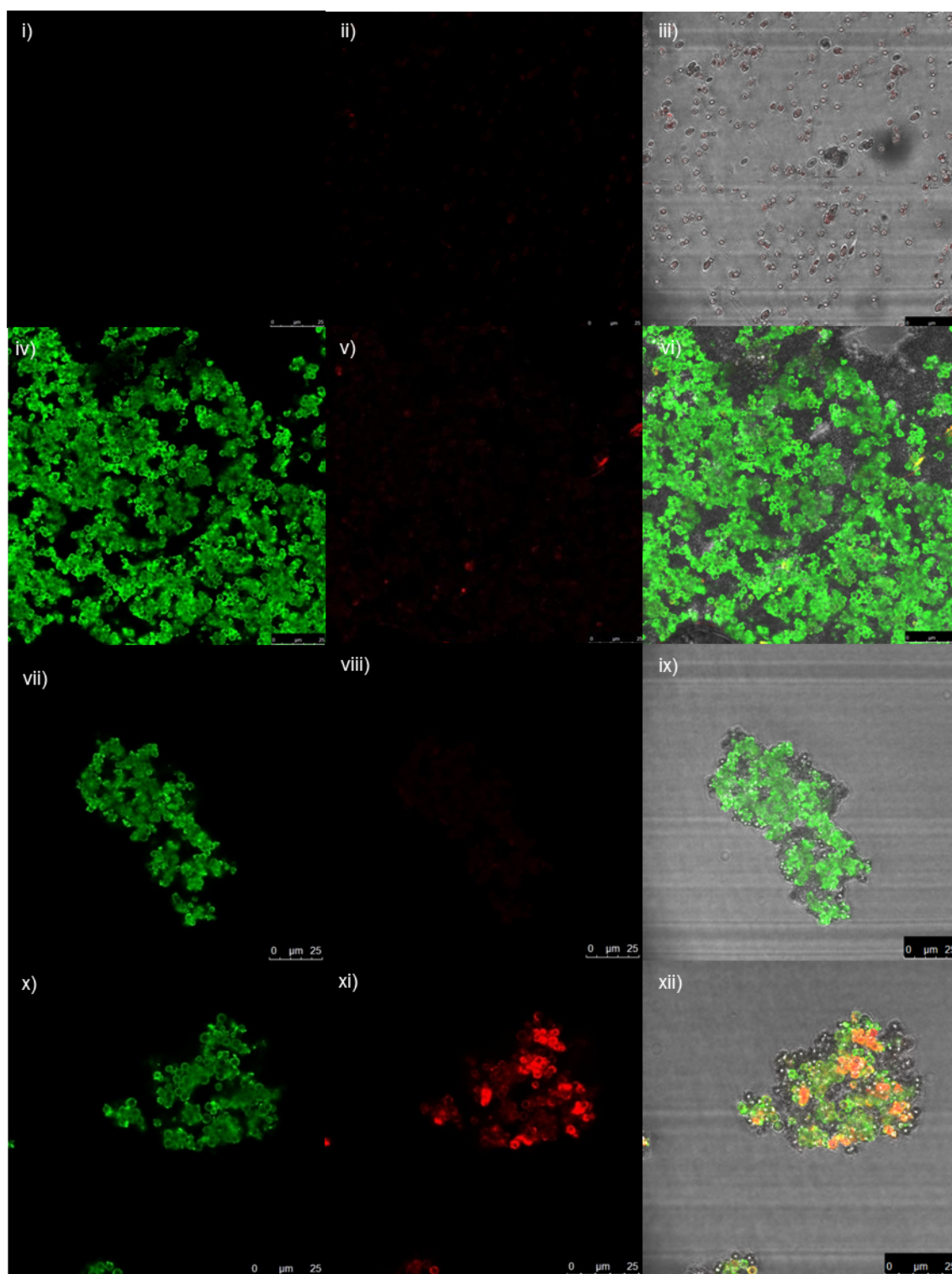


Figure S1. Fluorescence confocal microscopy images of microspheres subjected to EDAC coupling to BODIPY at various stages of the modification, to highlight the absence/presence of carboxylic acid groups on the outer surface of the microspheres. The 488 nm excitation laser was used at 15 % power, with 100x objective. Images i), ii) and iii) show trimethoxysilane-functionalised microspheres **2c**; iv), v) and vi) show amine-functionalised microspheres **3c**; vii), viii) and ix) show pyridyl-functionalised microspheres **4c**; and ix), xi)

and xii show carboxylic acid-functionalised microspheres **5c**. Left-hand images shows fluorescence emission collected in Channel 1 between 500 nm and 560 nm (FITC); central images shows fluorescence emission collected in Channel 2 between 590 nm and 630 nm (BODIPY); right hand images shows an overlay of Channels 1 and 2 and the phase Channel. Carboxylic acid- functionalised microspheres exhibit the only successful conjugation xi).

Quantifying amine functionality

The sol-gel process presents a facile way of altering the extent of amine-functionalisation of the silica shell. Simply increasing the amount of APTMS, up to at 1:1 ratio with TESO, incorporates an increased loading of amine groups. This was quantified by a two-step assay with amine-functionalised microspheres **3b**. Firstly, Fmoc-Lys-(Fmoc)-OH was conjugated to the amine groups. Secondly, the Fmoc moiety was cleaved with DBU and quantified by the characteristic absorbance at 294 and 305 nm of the cleavage product. These absorbance values were used to calculate the number of moles of cleaved Fmoc, and by extension the molar loading of our amine-functionalised microspheres. This strategy also exemplifies this microsphere system as a versatile template for covalent attachment of other desired compounds. Table S2 represents a series of amine-functionalised microspheres with increasing volume ratios of APTMS to TEOS. All other parameters were fixed. The ratio of silane to seed microspheres used for this assay was 2:1 ($\mu\text{l}:\text{mg}$) and the core seeds μ were not labelled with TR. Table S2 and Figure S2 confirm that an increased ratio of APTMS to TEOS gave a uniform increase in amine-loading up to a ratio of 1:1. Further increase in the relative amount of APTMS led to a reduction in the functional loading of the amine-functionalised microspheres. The assay confirms that the amine-loading can be tailored within a defined range.

Table S2. Amine-loading of amine-functionalised microspheres **3b** synthesised with increasing amounts of APTMS relative to TEOS.

Ratio of APTMS to TEOS/ $\mu\text{l}:\mu\text{l}$	Amine loading/ mmol g^{-1}
1:7	0.200
1:3	0.280
1:1	0.470
3:1	0.390
7:1	0.350

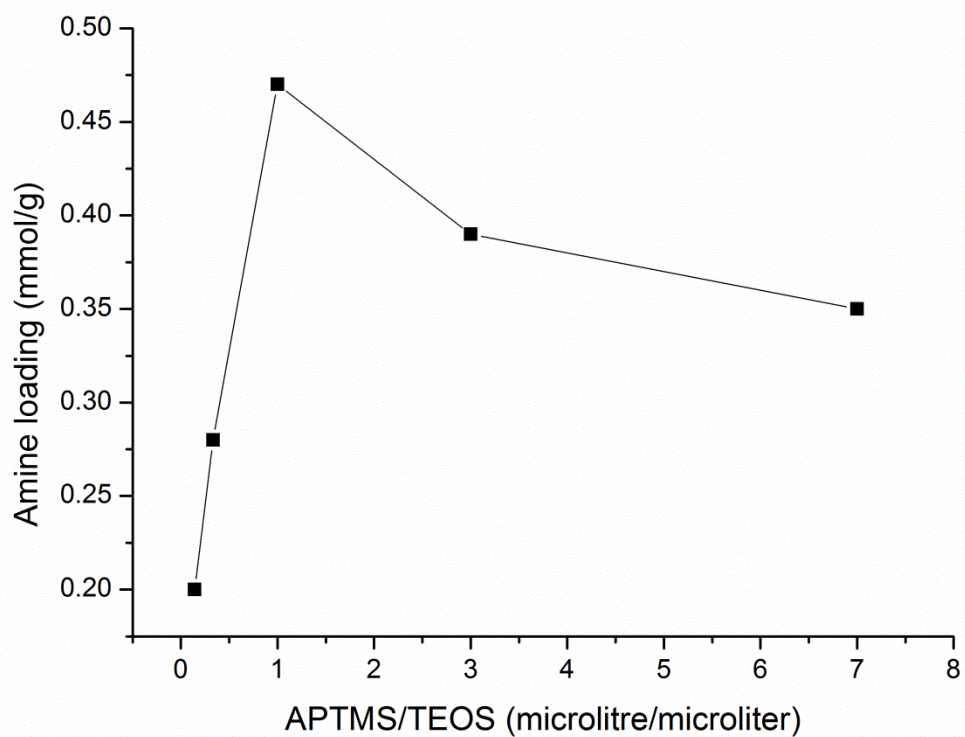


Figure S2. Amine-loading of amine-functionalised microspheres **3b** synthesised with increasing amounts of APTMS relative to TEOS.

IR spectroscopy

Trimethoxysilane-functionalised microspheres **2b** presented an ester C=O signal at 1723 cm^{-1} (a) corresponding to the methacrylate pendant groups, and two Si-O stretch signals at 1190 and 1088 cm^{-1} (b), which confirmed the presence of the poly(trimethoxysilyl propyl methacrylate) shell. The spectrum for amine-functionalised microspheres **3b** showed a subtle signal at 1618 cm^{-1} (c) corresponding to an N-H bend. Also, a marked increase in the intensity and broadness of the Si-O stretch signals at 1152 and 1065 cm^{-1} (d) confirmed the incorporation and polymerisation of TEOS and APTMS into the outer shell. Pyridyl-functionalised microspheres **4b** gave a strong stretching peaks at 1638 and 1618 cm^{-1} (e) typical of the pyridyl group, which was overwhelming compared to the Si-O stretch signals. The disappearance of those strong 1638 and 1618 cm^{-1} signals (f) for carboxylic acid-functionalised microspheres **5b** confirmed the exchange for the carboxylic acid group. For RNase-functionalised microspheres **6b**, the Si-O stretch signals no longer dominated the fingerprint region (g), which was more reminiscent of the many functional groups present in the protein.

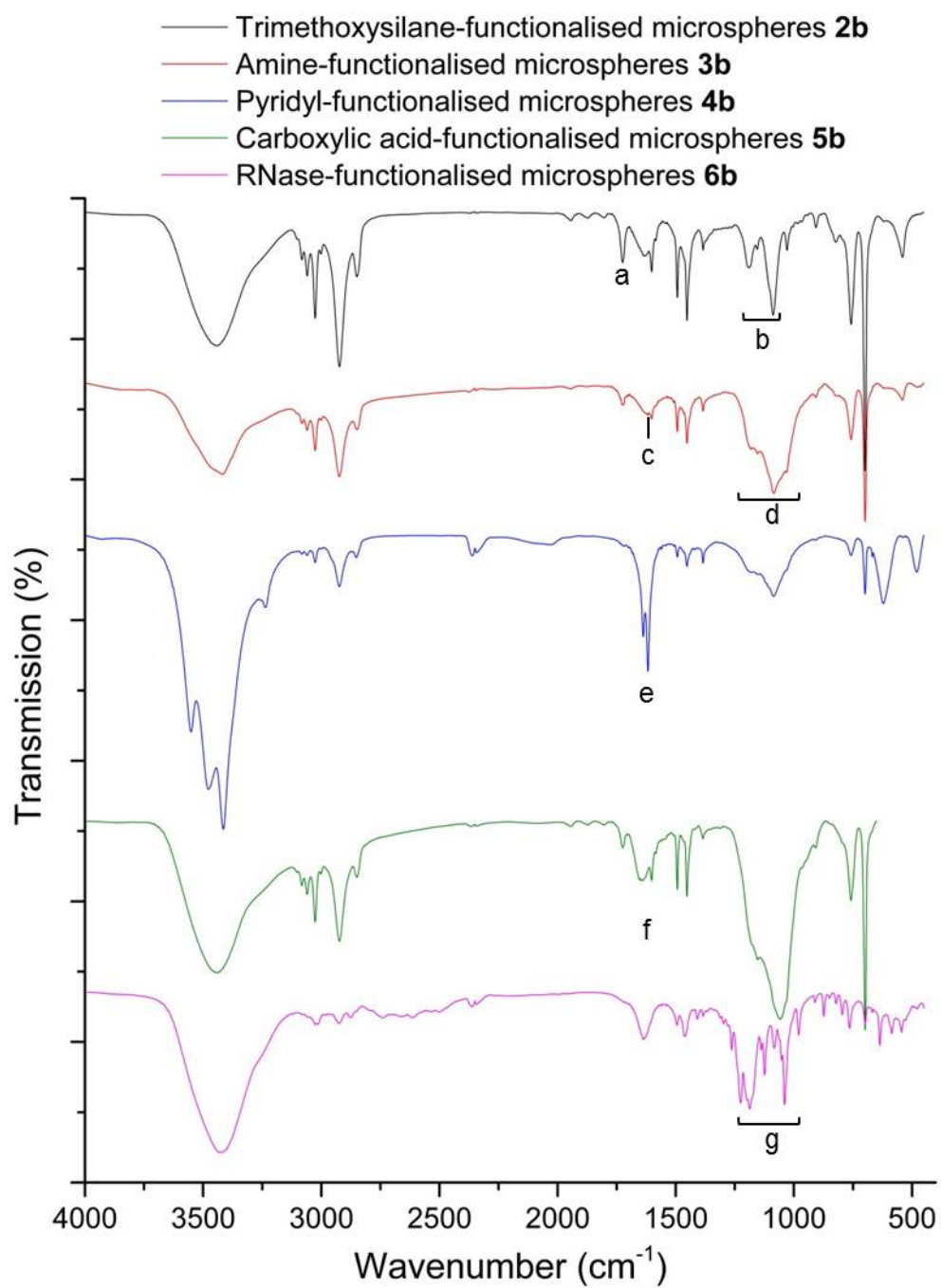


Figure S3. IR spectra of trimethoxysilane-functionalised microspheres **2b**, amine-functionalised microspheres **3b**, pyridyl-functionalised microspheres **4b**, carboxylic acid-functionalised microspheres **5b** and RNase-functionalised microspheres **6b**.

Control over silica shell thickness

Thiuronium-functionalised microspheres **1** were synthesised by dispersion polymerisation, and used as seed-particles in the seeded-emulsion polymerisation of the trimethoxysilane-functionalised shell **2b**. The resultant core-shell particles showed no increase in standard deviation (Table S3). Altering the amount of silane precursors, relative to the amount of seed-particles alters the thickness of the shell formed in a uniform fashion. This is true to a certain point, above which the sol-gel process produces aggregated microspheres. To demonstrate this, a series of sol-gel coatings were investigated, where the ratio of silanes (APTMS and TEOS combined) to trimethoxysilane-functionalised microspheres **2b** was doubled each time. Laser Diffractometry results are displayed in Table S3 and Figure S4. Although the standard deviations are high relative to the mean diameter of the microspheres, their consistency suggests that the sol-gel shell grows at the same rate on each particle.

Table S3. Size and distribution of microspheres measured by Laser Diffractometry.

Microspheres	Ratio of silanes to seed-particles/ $\mu\text{l}:\text{mg}$	Mean diameter/ μm	Standard deviation/ μm
Thiuronium-functionalised 1b	-	1.160	0.45
Trimethoxysilane-functionalised 2b	-	1.210	0.44
Amine-functionalised 3b	1:2	1.222	0.44 - 0.46
Amine-functionalised 3b	1:1	1.227	0.44 - 0.46
Amine-functionalised 3b	2:1	1.246	0.44 - 0.46
Amine-functionalised 3b	4:1	-	4.44

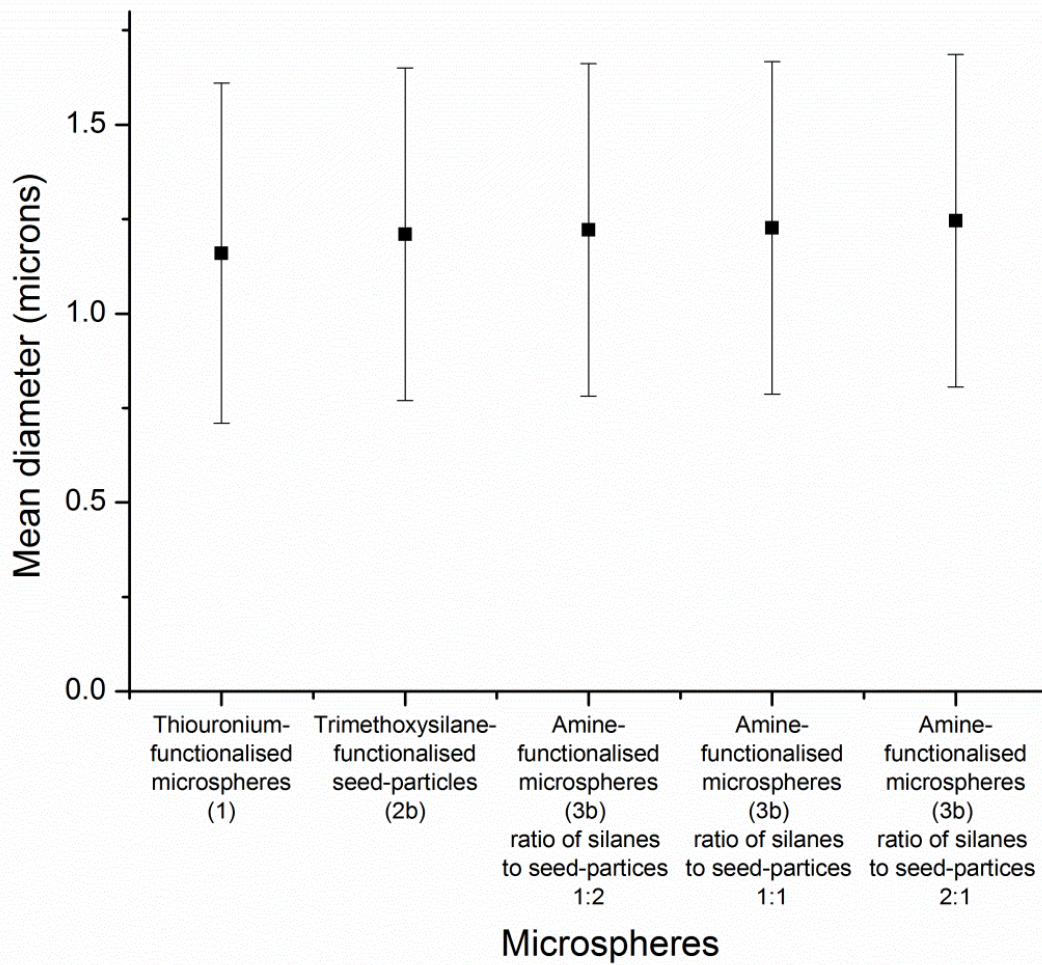


Figure S4. Mean particle diameter of silica-shelled microspheres synthesised with increasing amounts of silane precursors relative to seed particles.

TEM analysis

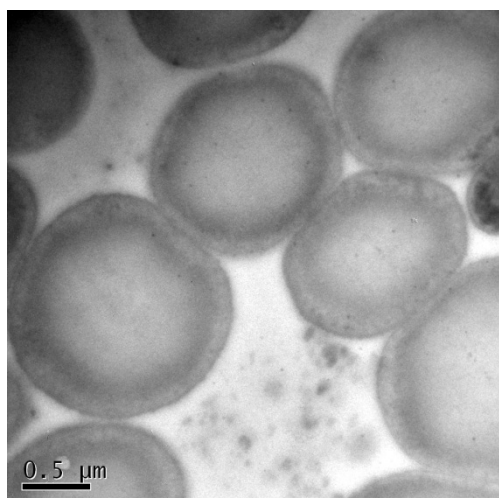


Figure S5. Transmission electron micrograph of amine-functionalised microspheres **3b** showing core-shell morphology (scale bar represents 0.5 μm).

EDXA data

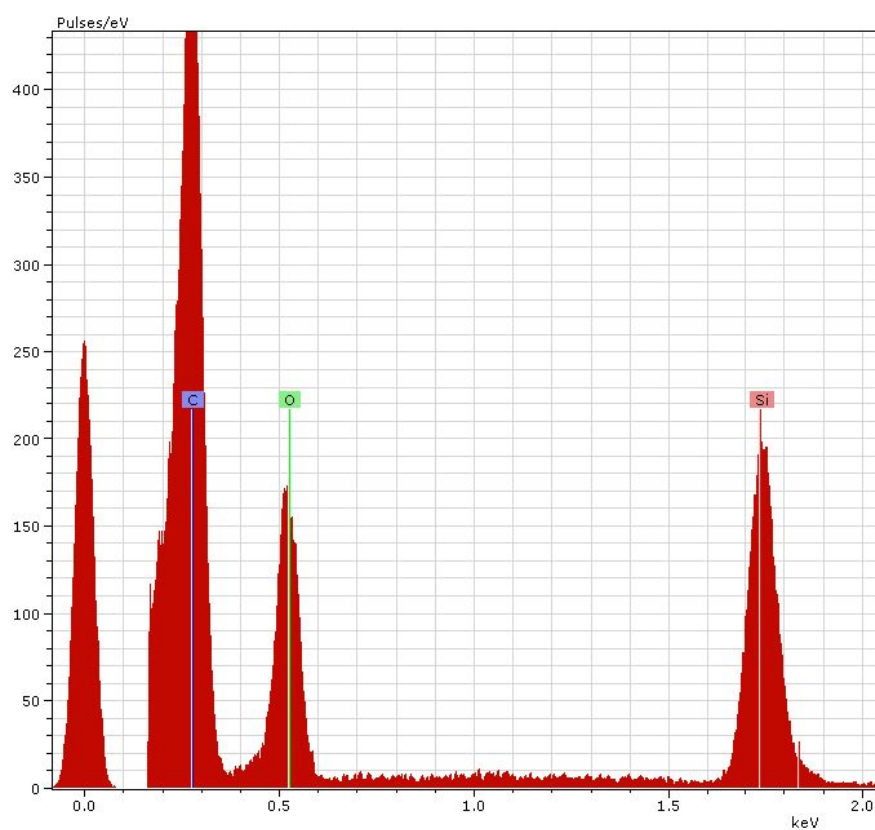


Figure S6. Energy dispersive x-ray analysis data of amine-functionalised microspheres **3b** showed high silica content.

Fluorescein isothiocyanate labelling of RNase

To verify the conjugation of RNase to microspheres, the peptide was labelled with fluorescein isothiocyanate (FITC, 389.38 g mol⁻¹) before conjugation. RNase A has a molecular weight of 13.7 kD and has 10 lysine residues and an amine at the N-terminus. RNase (2 mg, 1 x 10⁻⁷ mol) was dissolved in 0.1 M sodium carbonate buffer solution (2 ml). FITC in DMF (10 µg, 2.56 x 10⁻⁸ mol, in 10 µl) was added to the RNase solution with shaking in the dark at room temperature for 4 hours.

Control experiment to assess RNase coupling

Additional adsorption experiments and confocal fluorescence microscopy studies were conducted to verify that non-specific adsorption of RNase did not occur. Specifically, FITC-labelled RNase was incubated with microspheres under the same conditions as when it was coupled to the microspheres (for protocol see *EDAC coupling of RNase to carboxylic acid-functionalised microspheres* in the main manuscript) but this time without EDAC. No RNase was detected by confocal fluorescence microscopy confirming that the RNase does not adsorb onto the surface of the silica microspheres.



Figure S7. Confocal microscopy images of core-shell microspheres **5a** having TR (red)-labelled cores, unlabelled shells and having been incubated with FITC (green)-labelled RNase in the absence of EDAC. Images were obtained using a 488 nm excitation laser at 15 % power, and a 100× oil emersion objective with 12× zoom; i) fluorescence emission collected in Channel 1 between 590 nm and 630 nm, ii) fluorescence emission collected in Channel 2 between 500 nm and 560 nm, iii) overlay of Channel 1, Channel 2 and the phase channel.

Gel electrophoresis of RNase-FITC

The activity of RNase-FITC compared with pure RNase was investigated by gel electrophoresis. Degradation reactions with HeLa RNA resulted in the gel image displayed in Figures S6. Results show that RNase-FITC retains good degradative activity, but is slightly less than that of native RNase.

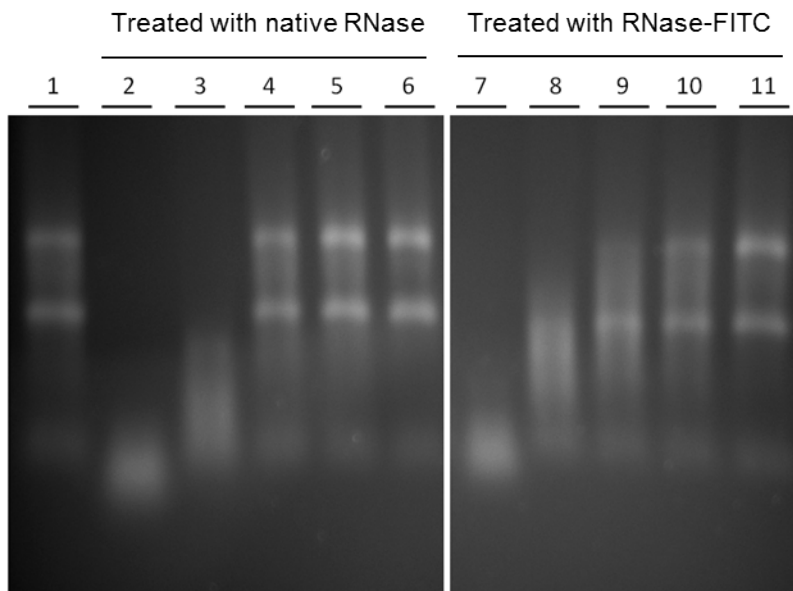


Figure S8. Gel electrophoresis to assess the activity of fluorescein-labelled RNase compared to native RNase. Each reaction was carried out with 1.5 μg of RNA for 3 minutes in a volume of 30 μl of 200 mM sodium acetate, 10 mM Tris HCl buffer (pH 7.5). Lane 1) control, no treatment, 2) 10^{-1} units of native RNase, 3) 10^{-2} units of native RNase, 4) 10^{-3} units of native RNase, 5) 10^{-4} units of native RNase, 6) 10^{-5} units of native RNase, 7) 10^{-1} units of RNase-FITC, 8) 10^{-2} units of RNase-FITC, 9) 10^{-3} units of RNase-FITC, 10) 10^{-4} units of RNase-FITC, 11) 10^{-5} units of RNase-FITC

Intensity profile analysis of degraded RNA (Figure 4, main paper)

The molecular weight profiles of HeLa RNA degraded either by native RNase or RNase-functionalised microspheres 6b were compared by examining the intensity profiles of products in each lane of the gel shown in Figure 4 (main paper). Best matches were overlaid (see below), indicating that there is close similarity in the RNase activity between 0.05 units of RNase (lane 4) / 1000 ng of microspheres (lane 7); 0.025 units of RNase (lane 5) / 100 ng of microspheres (lane 8) and 0.001 units of RNase (lane 6) / 10 ng of microspheres (lane 9). Note that activity is a function of both the quantity of immobilised enzyme and its accessibility to the RNA substrate. Lanes 1 (control) and 10 (1 ng of microspheres); lanes 2 & 3 contain RNA degraded by 0.01 and 0.075 units of native RNase respectively.

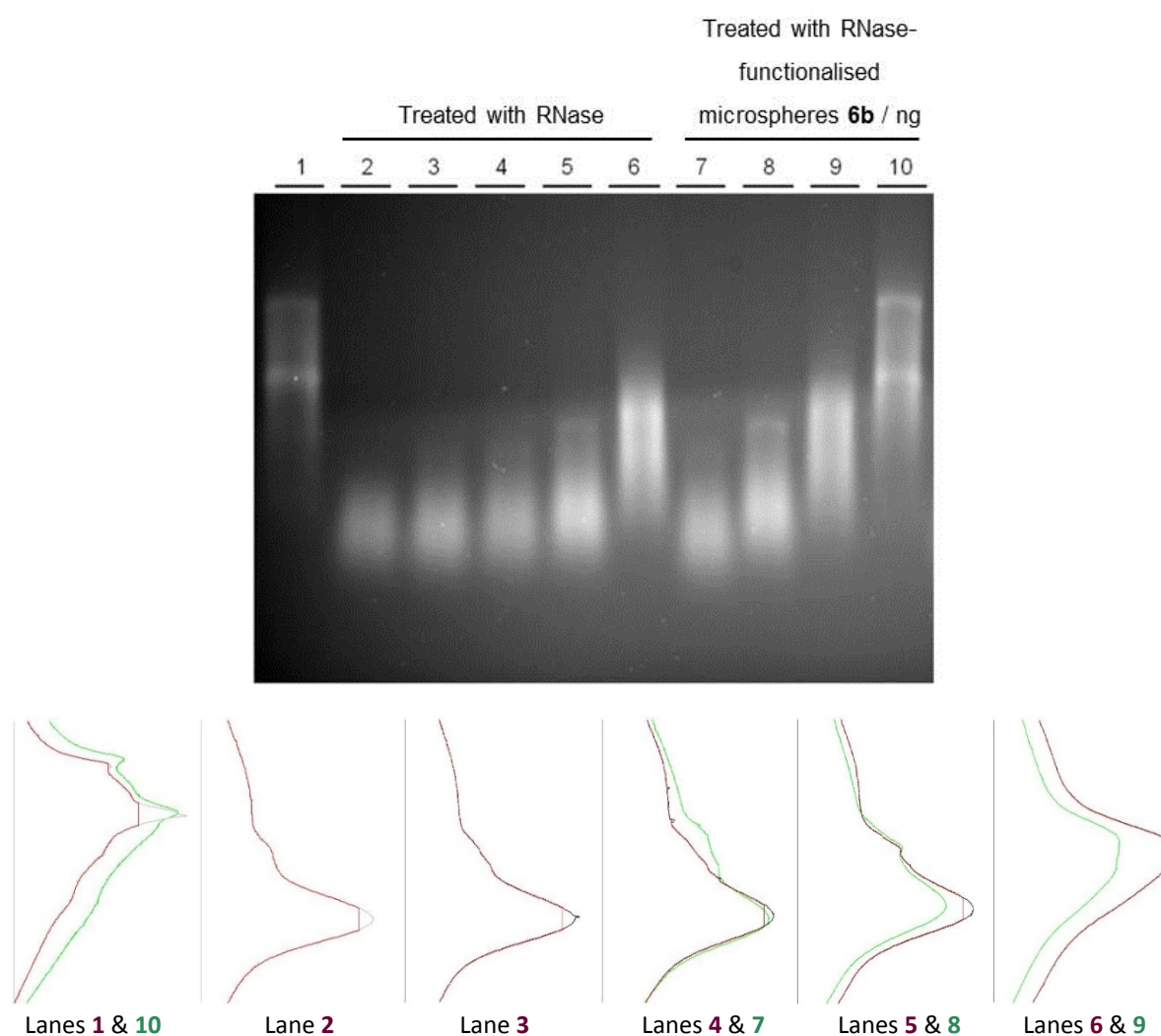


Figure S9 Intensity profiles of HeLa RNA degraded by native RNase are shown in red, whilst those degraded by RNase-functionalised microspheres 6b are shown in green.

Cellular delivery

In order to verify the internalisation of microspheres, adhered HeLa cells were incubated with RNase-functionalised microspheres without TR-labelled cores. After 36 hours, the cells were stained with PKH26 membrane stain *via* the protocol provided with the reagent (method not included) and suspended by trypsinising methods. Suspended cells were inspected by fluorescence confocal microscopy (Figure S7), and as expected RNase-functionalised microspheres were fully internalised by HeLa cells.

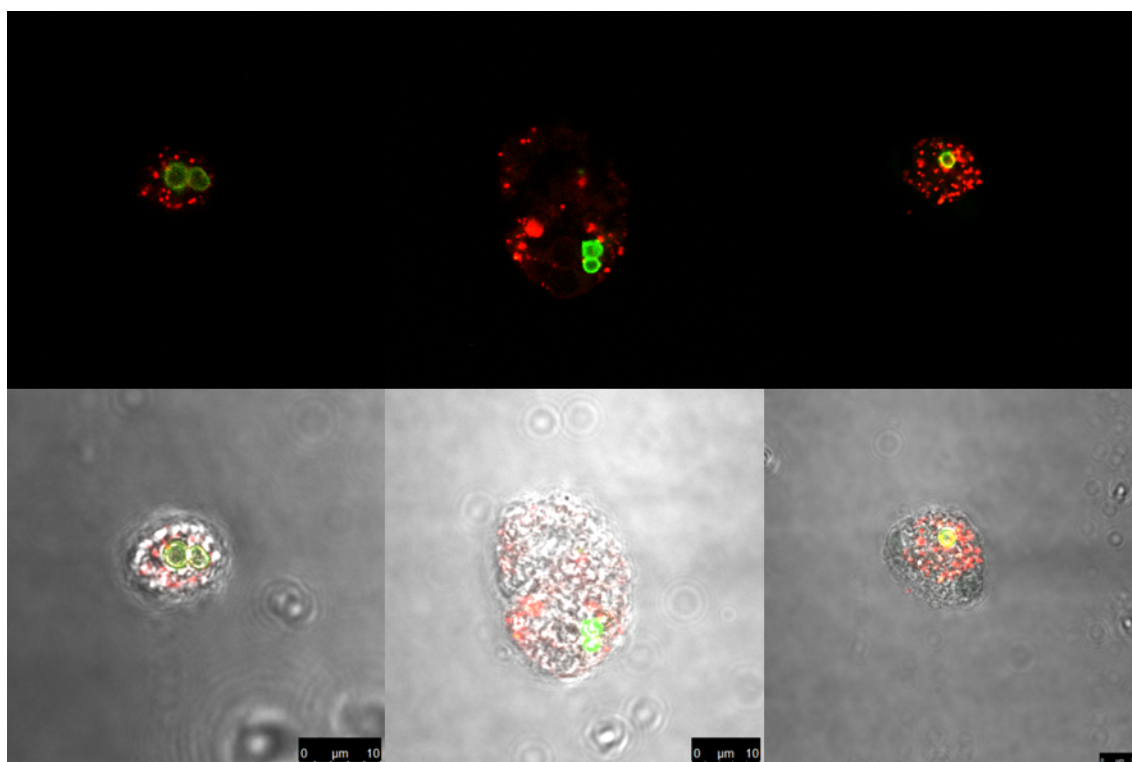


Figure S10. Fluorescence confocal microscopy images of HeLa cells in suspension, with internalised RNase-functionalised microspheres **6c**.